Colloids and Surfaces B: Biointerfaces 82 (2011) 359–364

Contents lists available at ScienceDirect

Colloids and Surfaces B: Biointerfaces

journal homepage: www.elsevier.com/locate/colsurfb

A hydrogen peroxide biosensor based on the direct electron transfer of hemoglobin encapsulated in liquid-crystalline cubic phase on electrode

Feng Gao[a,*], Zhen Yao[a], Qin'an Huang[b], Xiaoxiao Chen[a], Xinyin Guo[a], Qingqing Ye[a], Lun Wang[a]

[a] Anhui Key Laboratory of Chemo/Biosensing, Anhui Key Laboratory of Functional Molecular Solids, College of Chemistry and Materials Science, Anhui Normal University, Wuhu 241000, China
[b] Department of Basic Teaching, Wannan Medical College, Wuhu 241000, China

ARTICLE INFO

Article history:
Received 8 July 2010
Received in revised form 4 September 2010
Accepted 7 September 2010
Available online 21 September 2010

Keywords:
Cubic phase
Monoolein
Hemoglobin
Bioelectrocatalysis
Direct electron transfer
Biosensor
Hydrogen peroxide

ABSTRACT

Liquid crystal cubic phase formed with monoolein has been used as immobilizing matrix to host redox protein hemoglobin on glassy carbon electrode surface. The promoted direct electron transfer between hemoglobin and electrode was observed and a large average kinetic electron transfer rate constant k_s of 3.03(±0.02) s^{-1} was estimated. The electrode modified with cubic phase containing hemoglobin retains the bioactivity of hemoglobin and shows excellent bioelectrocatalytic activity to the reduction of hydrogen peroxide with a small apparent Michaelis–Menten constant of 0.25(±0.03) mM. A novel reagentless hydrogen peroxide biosensor was constructed using the hemoglobin-containing cubic phase modified electrode and the proposed hydrogen peroxide biosensor shows a linear range of 7.0–239 μM with a detection limit of 3.1(±0.2) μM and good stability and reproducibility.

1. Introduction

Since the very first two reports on direct electron transfer (DET) between cytochrome *c* and gold and tin doped indium oxides electrodes in 1977 by Hill [1] and Kuwana [2], respectively, DET reactions between native redox-active proteins/enzymes and electrodes have attracted considerable attention in the past several decades [3–5]. Studies on DET process of protein–electrode system not only can serve as a model system to give some information about the electron transfer mechanisms between proteins in biological and physiological systems, but also provide a platform without redox relays (mediators) for fabricating bioelectronic devices such as biosensors, bioreactors, biomotors, and biofuel cells. However, it is usually difficult to achieve the direct electron transfer between the redox proteins/enzymes and conventional bare electrodes due to some reasons including unfavorable orientation, long distance between redox center and electrode, and adsorption denaturation [6,7]. So, it is intriguing to develop suitable matrix to immobilize redox proteins/enzymes on electrode surface and, consequently, preserve the bioactivities of redox proteins/enzymes to make practical bioelectronic devices mentioned above.

A number of composite films such as nanomaterials [8–12], room temperature ionic liquids (RTIL) [13–17], surfactants [18–20], and clays [21–24] have been developed to incorporate redox proteins. Liquid-crystalline lipid cubic phase formed by polar lipids in aqueous media is one promising exception of model membranes, which is optically isotropic, highly viscous, thermodynamically stable in the laboratory for several months and easily prepared. Their internal structure consists of one congruent lipid bilayer, forming a three-dimensional and well-ordered structure interwoven by aqueous channels with a diameter about 5–6 nm. Moreover, they are stable in the presence of excess water [25–29]. From the bioelectrochemical point of view, these special characteristics make lipid cubic phase more preferable to host the biocatalysts (proteins or enzymes) on the electrode surface for electrochemical measurements in aqueous solution. For example, biocatalyst moleculars can be attached to the lipid moleculars and the high viscosity of cubic phase easily allows to fabricate the biosensing surface via casting biocatalyst-containing cubic phase mixture onto electrode surface, while the water channels will allow the enzyme substrates and products to diffuse freely through the cubic phase system. Cubic phase have already been successfully used to accommodate enzyme or synthetic catalysts on electrode surface [30–38]. Monoolein (1-monooleoyl-rac-glycerol, MO) is a typical example of

* Corresponding author at: Anhui Key Laboratory of Chemo/Biosensing, Anhui Key Laboratory of Functional Molecular Solids, College of Chemistry and Materials Science, Anhui Normal University, No. 1 Beijing East Road, Wuhu, Anhui Province 241000, China. Tel.: +86 553 3869302; fax: +86 553 3869302.
E-mail address: fgao@mail.ahnu.edu.cn (F. Gao).

0927-7765/$ – see front matter © 2010 Elsevier B.V. All rights reserved.
doi:10.1016/j.colsurfb.2010.09.009

a lipid forming such a cubic phase. It is highly viscous, transparent and at hydration over 20% is stable in contact with water [32–38].

Heme protein hemoglobin (Hb), which consists of four subunits of polypeptide enzymes, and a heme (iron porphyrin) group in each subunit acts as the active center. The electron transfer between a heme protein (e.g., myoglobin, hemoglobin) in solution and the bare electrode is either not observed or is very slow [39]. In this work, glassy carbon electrode covered by liquid-crystalline cubic phase formed by monoolein is proposed as the matrix for entrapping Hb and the DET between Hb and electrode is investigated. Based on its DET behavior and the bioelectrocatalysis activity to H_2O_2 reduction, a third-generation biosensor for H_2O_2 is established.

2. Experimental

2.1. Materials and chemicals

Monoolein (1-monooleoyl-rac-glycerol, 99%) was obtained from Sigma Chemical Co., hemoglobin (Hb) (Bovine blood, MW = 67,000) was purchased from J&K Chemical Ltd. and used as received. Hydrogen peroxide (H_2O_2, 30% w/w) solution was obtained from Shanghai Chemical Reagent Company (Shanghai, China). The dilute H_2O_2 solution was prepared daily. A 0.1 M phosphate buffer solution (pH 7.0) was used as supporting electrolyte and prepared by mixing the stock solutions of 0.1 M Na_2HPO_4 and KH_2PO_4. All other chemicals were of analytical grade and used without further purification. All solutions were prepared with double-distilled water.

2.2. Apparatus

All the electrochemical experiments were carried out on CHI660C potentiostat (CHI, Shanghai) with a conventional three-electrode cell. A glass carbon electrode or modified electrode was used as the working electrode, an Ag/AgCl as the reference electrode, and a platinum wire as the counter electrode. The experimental solutions were bubbled with highly pure nitrogen for 30 min to deoxygenate and kept under nitrogen atmosphere during the electrochemistry measurements. The electrochemical measurements were performed at room temperature and repeated minimum three times. Small angle X-ray diffraction (XRD) experiments were performed using a Shimadzu XRD-6000 X-ray diffractometer equipped with Cu Kα radiation ($\lambda = 0.154060$ nm) with a scanning rate of $0.02^\circ\ s^{-1}$ and 2θ ranges from 0.2° to 5°. A pH3-C pH meter (Shanghai, China) was used to adjust the desired pH value.

2.3. Preparation of monoolein cubic phase

The cubic phase was prepared by mixing monoolein (about 10 mg) and an appropriate amount of pure water or hemoglobin solution (2 mg/μL)in a centrifuge tube. The centrifuge tube was tightly sealed, followed by centrifugation for about 1 h at 4500 *g* for the contents to equilibrate. The ratio of the components was chosen according to the phase diagram for the monoolein–water system and it corresponds to a diamond type of cubic phase [25,32,40–42]. After centrifugation, a transparent, highly viscous and optically isotropic cubic phase was obtained. The cubic phase displays sanguine due to the color of hemoglobin.

2.4. Preparation of the Hb-cubic phase modified GC electrode

Prior to use, glassy carbon electrode (GC, ∅ = 3 mm) was polished on a polishing cloth with 0.3 and 0.05 μm alumina slurry, respectively. The electrode was carefully rinsed with double-distilled water and sonicated in ethanol and water for 2 min, respectively, and then let it dry at room temperature. The cubic phase was spread on the electrode surface using a spatula and the layer thickness was adjusted to 0.3 mm. In order to determine the exact amount of cubic phase on the electrode, the GC electrode was weighed before and after casting, and the amount was 5 mg. The electrode modified with cubic phase was immersed in the PBS which was deoxygenated and was kept in this solution for 20 min before each experiment to equilibrate the gas concentration between the cubic phase and solution.

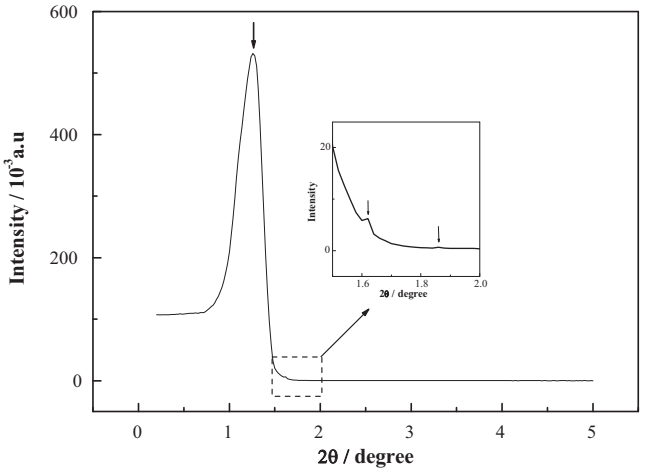

Fig. 1. Small-angle X-ray diffraction patterns of the MO–Hb–H_2O cubic phase system.

3. Result and discussion

3.1. Characterization of MO cubic phase

The phase behavior of MO cubic phase is well documented in literatures. MO forms reverse-type (i.e., water in oil) cubic phase structures in water. The formed phase are reversed isotropic and two types of liquid crystals (i.e., lamellar and cubic) are present. Two parts, corresponding to the biocontinuous structures of *Ia3d* and *Pn3m* symmetry, exist in the cubic phase domain of MO. Among these two structures, *Pn3m* structure exists only at high concentration of water (at high hydration level) and thus is stable in excess water, which is an important advantage for elaborating sensors of molecules present in water. At 20 °C, 44% water can be incorporated into the monoolein cubic phase, which allows an easy introduction of water-soluble moleculars such as protein/enzyme into liquid crystal matrix [25,30,32,40,41].

Hemoglobin-doped MO cubic phase was characterized with small-angle X-ray diffraction. One very strong diffraction peak at 2θ angle of 1.26° and two very weak peaks located at 1.64° and 1.81° are recorded in Fig. 1. According to Bragg equation ($2d \sin\theta = n\ \lambda$, $n = 1$), the Bragg reflections of the MO–Hb–H_2O system were indexed as (1 1 0), (2 0 0) and (2 1 1), and the corresponding Miller indices were 70.1, 53.8, and 49.1 Å, respectively. These X-ray diffraction data indicates that the cubic phase was the primitive cubic lattice of space group *Pn3m* [42–45], and the introduction of Hb does not change either the structure of the matrix or the lattice parameters values.

3.2. Direct electrochemistry of Hb immobilized in the lipid cubic phase

The cyclic voltammograms (CVs) of bare GC (a), MO/GC (b) and Hb–MO/GC (c) electrodes recorded in deoxygenated 0.1 M PBS (pH

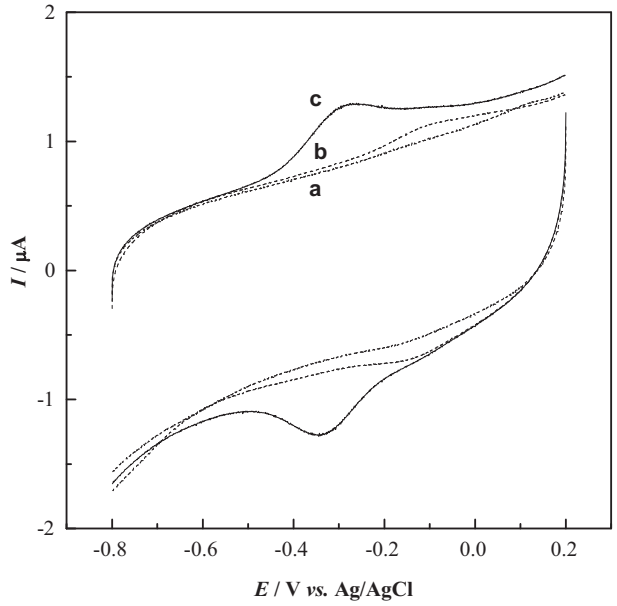

Fig. 2. Cyclic voltammograms of bare GC (a), MO/GC (b) and Hb–MO/GC (c) electrodes recorded in deoxygenated 0.1 M PBS (pH 7.0) with a scan rate of 200 mV/s.

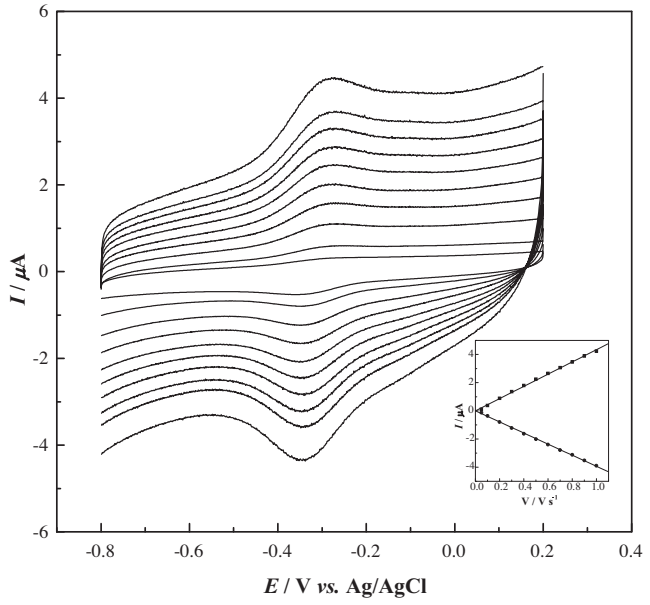

Fig. 3. Cyclic voltammograms of the Hb–MO/GC modified electrode in deoxygenated 0.1 M PBS (pH 7.0) at different scan rates. Scan rates (from inner to outer): 50, 100, 200, 300, 400, 500, 600, 700, 800, 900, 1000 mV s^{-1}. Inset: the plot of current against scan rate.

7.0) with a scan rate of 200 mV/s are shown in Fig. 2. At the MO cubic phase modified electrode (Fig. 2b), a pair of small redox peaks with an oxidation wave at 0.05 V and a reduction wave at −0.15 V are observed, which ascribes to the MO cubic phase layer and is a good agreement with previous literature [32]. When Hb is present in cubic phase (Fig. 2c), a well-defined and nearly symmetric redox peaks are observed. The cathodic and anodic peak potentials are −0.264 V and −0.344 V, respectively. The formal potential, $E^{0\prime}$ (defined as the average of anodic peak potential, E_{pa} and cathodic peak potential, E_{pc}) is −0.304 V (vs. Ag/AgCl) with a peak-to-peak separation (ΔE_p) of ca. 80 mV, which is consistent with the reported values for the Fe^{III}/Fe^{II} redox center of the heme group in Hb [9,16,46–48]. The results indicate that in cubic phase, the direct electron transfer between Hb and GC electrode is greatly enhanced.

The CVs of Hb–MO/GC electrode in deoxygenated PBS at different scan rates from 50 to 1000 mV s^{-1} are collected. As shown in Fig. 3, the anodic and cathodic peak potentials show little change and currents for the direct transfer reaction of Hb are linear with the increasing of scan rate (see inset in Fig. 3), indicating that Hb immobilized in cubic phase undergoes a reversible and surface-controlled electrochemical reaction process.

The interfacial electron transfer rate (k_s) of the Hb–MO/GC electrode can be estimated using the equation derived by Laviron for diffusionless cyclic voltammograms [49,50].

$$\log k_s = \alpha \log(1-\alpha) + (1-\alpha)\log\alpha - \log\left(\frac{RT}{nFv}\right) - \alpha(1-\alpha)\frac{nF\Delta E_p}{2.3RT}$$

The symbols R, T, and F have their usual meanings, n is the electron transfer number for Hb. Since the peak-to-peak separation (ΔE_p) was less than 200/n mV (as shown in Fig. 3), the electron transfer coefficient α is taken as 0.5. The average kinetic electron transfer rate constant k_s is estimated to be 3.03(±0.02) s^{-1}, which is larger than the value of 1.90 s^{-1} obtained for Hb/mesoTiO$_2$ modified electrode [51], 0.90 s^{-1} for polymer-Hb-MWNTs modified electrode [52], and 1.984 s^{-1} for gold colloid-silk fibroin modified electrode [48], indicating that the electron transfer rate of Hb entrapped in the cubic phase is fast. We attribute this enhanced electron transfer to the special structure of Hb–MO cubic phase system.

3.2.1. *Influence of solution pH on the DET of Hb*

The features of CVs of Hb–MO/GC electrode show a strong dependence on the pH of the electrolytic solution as shown in Fig. 4A. A couple of stable and well-defined redox peaks were obtained for entrapped Hb in PBS with different pH values ranging from 5.0 to 9.0. All changes in voltammetric peak potentials and currents with pH were reversible, that is, the same voltammogram can be obtained if the electrode is transferred from a solution with a different pH value back to its original solution. As shown in Fig. 4A, with pH increasing from 5.0 to 9.0, both the oxidation and reduction peaks potentials shift negatively. The formal potential showed linearly response to the solution pH (shown in Fig. 4B), suggesting the redox reaction was companied with protonated process. The slope was about −48.1 mV/pH, which is close to the expected value of 59 mV/pH calculated using the Nernst equation at 25 °C [53], and also in agreement with the reported values −45.2 [48], −51 [54], and −52 mV/pH [55]. Therefore, these values indicate that the proton diffusion in electron transfer reaction is fast, and also confirm single proton (H^+) and single electron (e^-) participate in the electron transfer process of Hb. The electron process can be described as following.

$$\text{Hbheme}(Fe^{III}) + H^+ + e^- = \text{Hbheme}(Fe^{II})$$

The results indicate that the MO cubic phase can provide a suitable microenvironment for the immobilized Hb.

3.2.2. *Electrocatalytic activity of Hb–MO/GC to the reduction of H_2O_2*

The electrocatalytic activity to the reduction H_2O_2 by the Hb–MO/GC electrode was investigated and characterized by cyclic voltammetry in deoxygenated 0.1 M PBS of pH 7.0 at a scan rate of 200 mV s^{-1}. As shown in Fig. 5, in the absence of H_2O_2, a pair of quasi-reversible and well-defined anodic and cathodic peaks was observed due to the direct electron transfer reaction between entrapped Hb and electrode. Once the addition of H_2O_2, a significant increase in the reduction peak at about −0.40 V was observed, while the oxidation peak current decreased simultaneously. Moreover, the reduction current increased gradually with the increasing

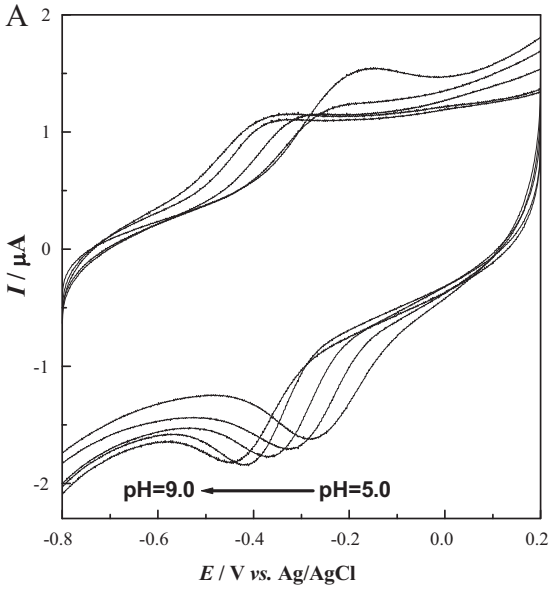

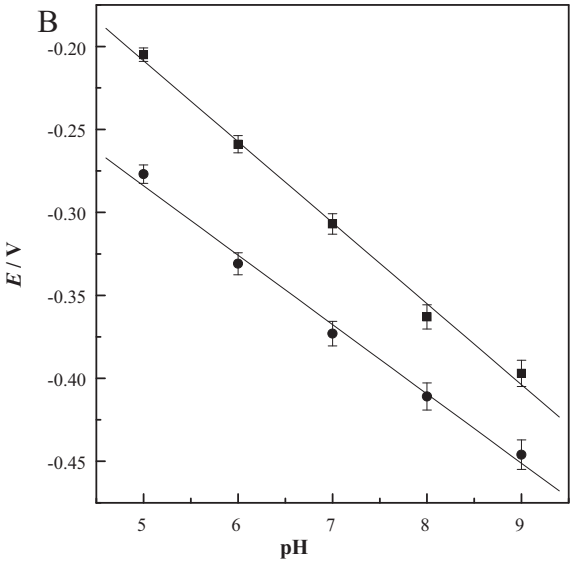

Fig. 4. CVs of a Hb–MO/GC electrode obtained in 0.1 M PBS with different pH values (from right to left: 5.0, 6.0, 7.0, 8.0, 9.0) at a scan rate of 200 mV s^{-1} (A). The relationship between the formal potentials and solution pH values (B). Error bars represent the range calculated using three different electrodes.

of H_2O_2 concentration. These results demonstrate a typical electrocatalytic reduction process of H_2O_2. The mechanism can be expressed as follows.

$$Hbheme(Fe^{III}) + H^+ + e^- = Hbheme(Fe^{II})$$

$$2Hbheme(Fe^{II}) + H_2O_2 \rightarrow 2Hbheme(Fe^{III}) + 2H_2O$$

Fig. 6 displays the amperometric response of Hb–MO/GC modified electrode to H_2O_2 with successive additions of H_2O_2 at an applied potential of −0.40 V to a continuous stirring deoxygenated PBS solution. Upon the addition of H_2O_2, the reduction current increased steeply within 15 s to reach a stable value and the reduction current increased linearly with H_2O_2 concentration. The response time for amperometric measurements was somewhat longer than some reported values, which maybe due to the different microenvironments of Hb present in the MO cubic phase, but this value is still comparable to that of 10 s reported for

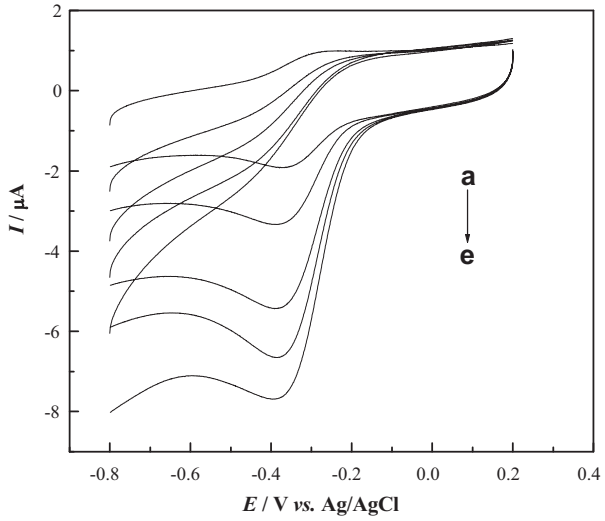

Fig. 5. Cyclic voltammograms of Hb–MO/GC in 0.1 M deoxygenated PBS (pH 7.0) containing H_2O_2 (from inner to outer): 0mM, 1.0, 2.0, 3.0, 4.0 mM.

Hb/Au–Zrp/Chitosan [47] and Hb/CMC-TiO_2-NT electrodes [56], and 15 s reported for hemoglobin immobilized on colloidal gold-hydroxyapatite nanocomposite [57], and this value is also better than 20 s for sol–gel-derived amperometric biosensor for H_2O_2 [58], 30 s for graphite-based H_2O_2 biosensor [59], and 20 s for H_2O_2 biosensor with montmorillonite-modified bovine serum albumin (BSA)–glutaraldehyde as matrix [60]. The calibration curve for H_2O_2 detection is shown in the inset A of Fig. 6 and the linear response ranges from 7×10^{-6} to 2.39×10^{-4} M with a correlation coefficient of 0.9992 ($n = 21$). The detection limit was estimated to be 3.1(±0.2) μM at a signal-to-noise ratio of 3. The sensitivity of the electrode was found to be 294 nA/mM. The comparative results of some analytical parameters for different H_2O_2 biosensors were listed in Table 1. As shown in Table 1, the analytical parameters for the present H_2O_2 biosensor are comparable or better than the results reported for different H_2O_2 biosensors.

When the concentration of H_2O_2 increases gradually, a response plateau is observed, showing the typical characteristics of Michaelis–Menten kinetic mechanism. The apparent Michaelis–Menten constant (K_M^{app}) is a characteristic of the film on the electrode, not of the enzyme, and usually differs substaintially

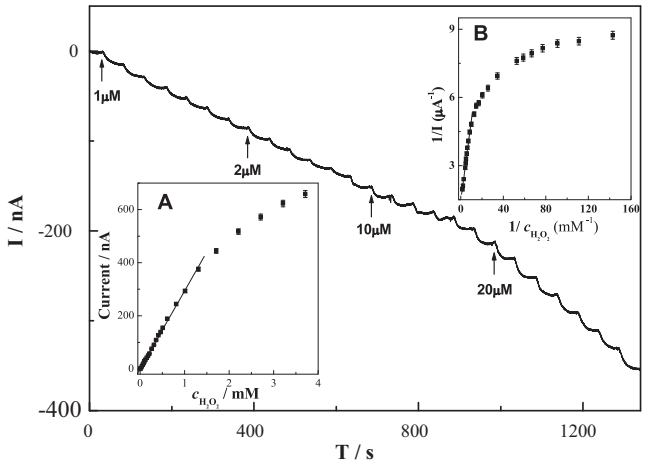

Fig. 6. Amperometric response of Hb–MO/GC electrode upon successive additions of H_2O_2 in 0.1 M deoxygenated PBS (pH 7.0) at −0.40 V. Inset A: the corresponding calibration plot. Inset B: the plot of $1/I_{ss}$ against $1/c$. Error bars represent the range calculated using three different electrodes.

Table 1
Comparison of analytical parameters for different hydrogen peroxide sensors based on the EDT of Hb.

Electrode	Linear range (μM)	Detection limit (μM)	Reference
Hb/MO	7.0–239	3.1	This work
Hb/CMC-TiO_2-NT	4–64	4.637	[56]
Hb/graphene/chitosan	6.5–230	0.51	[46]
Hb/Au–Zrp/chitosan	15–480	7.4	[47]
Hb/PAA	20–250	0.2	[61]
Hb/IL	1–52	7	[62]
Hb/HMS	0.4–6	0.018	[63]
Hb/PC	10–100	3.9	[64]
Hb/ZrO_2/DMSO	1.5–30.2	0.14	[65]
Hb/NGC-SF	600–1700	100	[48]
Hb/PTFE	1.26–10.08	–	[66]
Hb/TATP	19.58–117.48	22.61	[67]

CMC, carboxymethyl cellulose; Zrp, α-zirconium phosphate; PAA, poly-allylamine; IL, ionic liquid; HMS, hexagonal mesoporous silica; PC, phosphatidylcholine; DMSO, dimethyl sulfoxide; NGC-SF, nanostructured gold colloid-silk fibroin; PTFE, polytetrafluoroethylene; TATP, triacetone triperoxide.

from the enzyme constant, measured in a homogenous solution. The apparent Michaelis–Menten constant can be obtained from the electrochemical version of Lineweaver–Burk equation [68]:

$$\frac{1}{I_{ss}} = \frac{1}{I_{max}} + \frac{K_M^{app}}{I_{max}c}$$

Here, I_{ss} is the steady-state current after the addition of substrate, which can be obtained from the amperometric experiments, I_{max} is the maximum current under saturated substract condition and c is the bulk concentration of the substrate. From the slope of the plot of $1/I_{ss}$ against $1/c$ as shown in the inset B of Fig. 6, the apparent Michaelis–Menten constant is calculated to be 0.25(±0.03) mM. This value is much smaller than that reported for the Hb immobilized onto the surface of carbon nanotube of 41 mM [69], Hb immobilized on Au–Zrp of 0.65 mM [47], SP dephadex membrane of 1.9 mM [70]. The low value of the apparent Michaelis–Menten constant indicates that Hb entrapped into the cubic phase retains its high bioactivity and has a much better affinity to H_2O_2.

3.2.3. Stability and reproducibility of the H_2O_2 biosensor

The storage stability of the electrode was investigated by monitoring its response to 100 μM H_2O_2. A ca. 6.8% decrease of initial current was observed after the storage of two weeks. The operational stability of the electrode was also examined by successive assays of 100 μM H_2O_2 using one same Hb–MO/GC electrode. The electrode was regenerated by immersing in pH 7.0 phosphate buffer after each of the measurements. The reproducible current with a R.S.D. value of 3.7% was obtained for 13 successive assays. The reproducibility between five Hb–MO/GC electrodes fabricated independently with the same way was also investigated. The five electrodes were used for the measurements of 100 μM H_2O_2 and show a satisfactory R.S.D. of 3.1%. The good stability and reproducibility may be attributed to the stable entrapment of Hb in cubic phase.

3.2.4. Interference determination of foreign substances

The effect of common interference substance, such as ascorbic acid, uric acid, glucose, and some amino acids on H_2O_2 determination was also investigated. The results showed that these substances did not show significant interfering to the determination of H_2O_2. These results indicate that the Hb–MO/GC electrode possess potential application for H_2O_2 biosensor.

4. Conclusions

In the present work, the monoolein-based cubic phase matrix was successfully used for the immobilization of Hb on the electrode surface. The entrapped Hb in cubic phase retains its high bioactivity and shows good affinity to H_2O_2 due to the unique properties of reverse biocontinuous cubic phase, which provides a suitable microenviroment for stabilization of the protein structure. The results in the present work demonstrate that use of cubic phase as matrix for proteins/enzymes entrapment is an attractive alternative to other immobilization methods and the preparation of proteins/enzymes-containing cubic phase is extremely simple, which is important for practical application.

Acknowledgements

F. Gao is grateful for the financial support from the Natural Science Foundation of China (Grant Nos. 20705001, 21005003), the Key Project of Educational Committee of Anhui Province (Grant No. KJ2007A008), and Starting Foundation for PhD of Anhui Normal University. Q. Huang also thanks the Project of Educational Committee of Anhui Province (Grant No. KJ2010B240) for its financial support.

References

[1] E.J. Eddowes, H.A.O. Hill, J. Chem. Soc., Chem. Commun. (1977) 771.
[2] P. Yeh, T. Kuwana, Chem. Lett. (1977) 1145.
[3] J.A. Cracknell, K.A. Vincent, F.A. Armstrong, Chem. Rev. 108 (2008) 2439.
[4] L. Gorton, A. Lindgren, T. Larrson, F.D. Munteanu, T. Ruzgas, I. Gazaryan, Anal. Chim. Acta 400 (1999) 91.
[5] N. Hu, Pure Appl. Chem. 73 (2001) 1979.
[6] J.F. Rusling, Acc. Chem. Res. 31 (1998) 363.
[7] A. Heller, Acc. Chem. Res. 23 (1990) 128.
[8] Y. Zhao, Y. Bi, W. Zhang, Q. Luo, Talanta 65 (2005) 489.
[9] X. Han, W. Cheng, Z. Zhang, S. Dong, E. Wang, Biochim. Biophys. Acta 1556 (2002) 273.
[10] Y. Liu, R. Yuan, Y. Chai, D. Tang, J. Dai, X. Zhong, Sens. Actuators B: Chem. 115 (2006) 109.
[11] C.A. Paddon, F. Marken, Electrochem. Commun. 6 (2004) 1249.
[12] A. Liu, M. Wei, I. Honma, H. Zhou, Anal. Chem. 77 (2005) 8068.
[13] X. Lu, J. Hu, X. Yao, Z. Wang, J. Li, Biomacromolecules 7 (2006) 975.
[14] A. Safavi, N. Maleki, O. Moradlou, M. Sorouri, Electrochem. Commun. 10 (2008) 420.
[15] G. Li, L. Du, H. Chen, L. Zhang, E. Wang, Electroanalysis 20 (2008) 2171.
[16] Y. Zhang, R. Yan, F. Zhao, B. Zeng, Colloids Surf., B 71 (2009) 288.
[17] Y. Li, X. Zeng, X. Liu, X. Liu, W. Wei, S. Luo, Colloids Surf., B 79 (2010) 241.
[18] J.F. Rusling, A.E.F. Nassar, J. Am. Chem. Soc. 115 (1993) 11891.
[19] J. Yang, N. Hu, Biosens. Bioelectron. 48 (1999) 117.
[20] F. Wang, S. Hu, Colloids Surf., B 63 (2008) 262.
[21] M. Li, S. Chen, F. Ni, Y. Wang, L. Wang, Electrochim. Acta 53 (2008) 7255.
[22] K. Charradi, C. Forano, V. Prevot, A.B.H. Amara, C. Mousty, Langmuir 25 (2009) 10376.
[23] Y. Zhou, N. Hu, Y. Zeng, J.F. Rusling, Langmuir 18 (2002) 211.
[24] Z. Li, N. Hu, J. Electroanal. Chem. 558 (2003) 155.
[25] S.T. Hyde, S. Anderson, B. Ericsson, K.Z. Larsson, Kristallograhie 168 (1984) 213.
[26] P. Nollert, A. Royant, E. Pebay-Peyroula, E.M. Landau, FEBS Lett. 457 (1999) 205.
[27] S. Engstrom, T.P. Norden, H. Nyquist, Eur. J. Pharm. Sci. 8 (1999) 243.
[28] R. Koynova, M. Caffrey, Chem. Phys. Lipids 115 (2002) 107.
[29] T. Nylander, C. Mattisson, V. Razumas, Y. Miezis, B. Hfikansson, Colloids Surf., A 114 (1996) 311.
[30] V. Razumas, J. Kanapienienė, T. Nylander, S. Engström, K. Larsson, Anal. Chim. Acta 289 (1994) 155.
[31] M. Popers, R. Bilewicz, M. Stébé, A. Hamidi, A. Miclo, E. Rogalska, Phys. Chem. Chem. Phys. 3 (2001) 240.
[32] P. Rowiński, R. Bilewicz, M.J. Stébé, E. Rogalska, Anal. Chem. 76 (2004) 283.
[33] E. Nazaruk, A. Michota, J. Bukowska, S. Shleev, L. Gorton, R. Bilewicz, J. Biol. Inorg. Chem. 12 (2007) 335.
[34] E. Nazaruk, R. Bilewicz, G. Lindblom, B. Lindholm-Sethson, Anal. Bioanal. Chem. 391 (2008) 1569.
[35] P. Rowiński, R. Bilewicz, M.J. Stébé, E. Rogalska, Anal. Chem. 74 (2002) 1554.
[36] P. Rowinski, C. Kang, H. Shin, A. Heller, Anal. Chem. 79 (2007) 1173.
[37] E. Nazaruk, K. Sadowska, K. Madrak, J.F. Biernat, J. Rogalsko, R. Bilewicz, Electroanalysis 21 (2009) 507.
[38] E. Rogalska, S. Smolinski, M. Swatko-Ossor, G. Ginalska, J. Fiedurek, J. Rogalski, R. Bilewicz, J. Power Sources 183 (2008) 533.
[39] I. Taniguchi, K. Watanabe, M. Tominaga, F.M. Hawkridge, J. Electroanal. Chem. 333 (1992) 331.

[40] K. Larsson, J. Phys. Chem. 93 (1989) 7304.
[41] P.O. Eriksson, G. Lindblom, Biophys. J. 64 (1993) 129.
[42] S.B. Leslie, S. Puvvada, B.R. Ratna, A.S. Rudolph, Biochim. Biophys. Acta 1285 (1996) 246.
[43] K. Larsson, Y. Miezis, T. Nylander, J. Phys. Chem. 100 (1996) 11766.
[44] J. Kraineva, R.A. Narayanan, E. Kondrashkina, P. Thiyagarajan, R. Winter, Langmuir 21 (2005) 3559.
[45] G. Rummel, A. Hardmeyer, C. Widmer, M.L. Chiu, P. Nollert, K.P. Locher, I. Pedruzzi, E.M. Landau, J.P. Rosenbusch, J. Struct. Biol. 121 (1998) 82.
[46] H. Xu, H. Dai, G. Chen, Talanta 81 (2010) 334.
[47] J. Feng, J. Xu, H. Chen, J. Electroanal. Chem. 585 (2005) 44.
[48] H. Guo, D. Liu, X. Yu, X. Xia, Sens. Actuators B: Chem. 139 (2009) 598.
[49] E. Laviron, J. Electroanal. Chem. 101 (1979) 19.
[50] E. Laviron, L. Roullier, J. Electroanal. Chem. 115 (1980) 65.
[51] N. Jia, Y. Wen, G. Yang, Q. Lian, C. Xu, H. Shen, Electrochem. Commun. 10 (2008) 774.
[52] L. Chen, G. Lu, J. Electroanal. Chem. 597 (2006) 51.
[53] A.J. Bard, L.R. Faulkner, Electrochemical Methods: Fundamentals and Applications, John Wiley and Sons, New York, 2001.
[54] C.H. Wang, C. Yang, Y.Y. Song, W. Gao, X.H. Xia, Adv. Funct. Mater. 15 (2005) 1267.
[55] H. Yao, N. Li, J.Z. Xu, J.J. Zhu, Talanta 71 (2007) 550.
[56] W. Zheng, Y.F. Zheng, K.W. Jin, N. Wang, Talanta 74 (2008) 1414.
[57] J. You, W. Ding, S. Ding, H. Ju, Electroanalysis 21 (2009) 190.
[58] B. Wang, S. Dong, Talanta 51 (2000) 565.
[59] P. Pandey, S. Upadhyay, I. Tiwari, V. Tripathi, Sens. Actuators B: Chem. 72 (2001) 224.
[60] C. Lei, J. Deng, Anal. Chem. 68 (1996) 3344.
[61] A.K.M. Kafi, D. Lee, S. Park, Y. Kwon, Thin Solid Films 515 (2007) 5179.
[62] Y. Wen, X. Yang, G. Hu, S. Chen, N. Jia, Electrochim. Acta 54 (2008) 744.
[63] Z. Dai, S. Liu, H. Ju, H. Chen, Biosens. Bioelectron. 19 (2004) 861.
[64] X. Han, W. Huang, J. Jia, S. Dong, E. Wang, Biosens. Bioelectron. 17 (2002) 741.
[65] S. Liu, Z. Dai, H. Chen, H. Ju, Biosens. Bioelectron. 19 (2004) 963.
[66] Q. Lu, S. Hu, Chem. Phys. Lett. 424 (2006) 167.
[67] F. Jian, Y. Qiao, R. Zhuang, Sens. Actuators B: Chem. 124 (2007) 413.
[68] R.A. Kamin, G.S. Willson, Anal. Chem. 52 (1980) 1198.
[69] C. Cai, C. Chen, Anal. Biochem. 325 (2004) 285.
[70] C.H. Fan, H.Y. Wang, S. Sun, D.X. Zhu, G. Wagner, G.X. Li, Anal. Chem. 73 (2001) 2850.